

## Structure of the moving piezoelectric polaron

John Thomchick and George Whitfield

*Department of Physics, Pennsylvania State University, University Park, Pennsylvania 16802*

(Received 27 June 1974)

Both the intermediate-coupling theory and a strong-coupling theory appropriate for a moving polaron give an anomalous energy-momentum relation,  $E(P)$ , for the piezoelectric polaron. This relation starts out quadratic at small  $P$ , but at large  $P$  it asymptotes to a straight line with slope equal to the speed of sound  $s$ . It is shown that the states represented by this anomalous  $E$  vs.  $P$  relation are such that the electron is clothed by its concomitant lattice distortion and that this lattice distortion becomes larger as the polaron velocity  $v \rightarrow s$ . This indicates that in this limit an increasing number of phonons are gathering in the "phonon cloud" around the electron. In both theories the constant lattice-potential surfaces become flattened in the forward and backward directions as the polaron starts to move.

### I. INTRODUCTION

In a recent series of papers<sup>1-6</sup> it has been argued that the piezoelectric polaron obeys an anomalous energy-momentum relation  $E(P)$ . The  $E$ -vs- $P$  curve which is thought to be correct starts out quadratic at small  $P$ , but at large  $P$  asymptotes to a straight line with slope equal to the speed of sound  $s$ . This behavior is predicted by energy-level crossing arguments<sup>1,7</sup> which consider the degeneracy inherent in the system of non-interacting conduction-band electron and acoustic phonons. The electron-phonon interaction causes the degenerate states to split, leaving the lowest state of the system with the anomalous  $E$ -vs- $P$  relation described above. Both the intermediate-coupling theory<sup>8,9</sup> and a version of strong-coupling theory appropriate for a moving polaron<sup>10</sup> yield this type of anomalous behavior.<sup>1,2</sup> For the intermediate-coupling theory, it has been shown that neither the inclusion of anisotropy<sup>3</sup> nor the introduction of a screened interaction<sup>4</sup> cause this anomalous behavior to disappear and that this behavior persists even at finite temperatures.<sup>5</sup>

However, the anomalous  $E(P)$  relation at large  $P$  is similar to the curve for a free acoustic phonon and this suggests that the states giving the anomaly may be composed of a slow electron plus a free acoustic phonon with momentum  $\approx P$ . If this were the case these states should not be thought of as polarons.

A quite different physical picture and one which is supported by the calculations in this paper is that as the electron approaches the speed of sound the electron-phonon interaction becomes strengthened because of the degeneracy. This causes an increasing number of acoustic phonons to take part in forming the lattice distortion around the electron. The large lattice distortion then traps the electron preventing it from traveling faster than the speed of sound.

In Sec. II of this paper we calculate the potential caused by the lattice distortion around the electron. We calculate the potential rather than the strain tensor because it is much simpler and still illustrates what we want to know. We find that as the polaron velocity  $v \rightarrow s$  the lattice potential around the electron deepens indicating that the lattice distortion grows larger in this limit. This result contradicts the naive expectation that the polaron should shed its "phonon clothing" as it starts to move and agrees with the physical picture described in the preceding paragraph.

### II. LATTICE POTENTIAL

In a spherically symmetric formulation the Fröhlich Hamiltonian for the piezoelectric polaron is

$$H = H_e + H_{ph} + H_{int}, \quad (1a)$$

where

$$H_e = \frac{1}{2} p^2; \quad (1b)$$

$$H_{ph} = \sum_{\vec{q}} \omega_q a_{\vec{q}}^\dagger a_{\vec{q}}, \quad \omega_q = q; \quad (1c)$$

and

$$H_{int} = \sum_{\vec{q}} Q(q) (a_{\vec{q}} + a_{-\vec{q}}^\dagger) e^{i\vec{q} \cdot \vec{r}_e}, \quad Q(q) = \left( \frac{4\pi\alpha}{\mathcal{V}q} \right)^{1/2}. \quad (1d)$$

The electron coordinate and momentum operators are  $\vec{r}_e$  and  $\vec{p}$ . The operators  $a_{\vec{q}}^\dagger$  create and annihilate phonons of an effective acoustic mode  $\vec{q}$ . The volume is  $\mathcal{V}$  and  $\alpha$  is the effective coupling constant.<sup>3,11,12</sup> The units are such that  $\hbar = m = s = 1$ , where  $m$  is the conduction band mass and  $s$  is the speed of sound.

The interaction term, Eq. (1d), is just the potential energy of the electron in the polarization field of the lattice. Thus, except for a factor of

electronic charge  $e$ , the lattice potential at  $\vec{r}_e$  is given by  $H_{\text{int}}$ .

#### A. Strong-coupling theory

The trial wave function used in strong coupling is<sup>2</sup>

$$|\psi_{\text{sc}}\rangle = e^{i\vec{W}\cdot\vec{r}_e} \phi(\vec{r}_e - \vec{r}) e^{S(\vec{r})} |0\rangle. \quad (2)$$

The lattice part of the wave function  $e^{S(\vec{r})} |0\rangle$  describes a lattice distortion centered about the point  $\vec{r}$ . The operator  $S(\vec{r})$  is given by

$$S(\vec{r}) = \sum_{\vec{q}} d_{\vec{q}} (a_{\vec{q}} e^{i\vec{q}\cdot\vec{r}} - a_{\vec{q}}^\dagger e^{-i\vec{q}\cdot\vec{r}}). \quad (3)$$

The parameter  $d_{\vec{q}}$  is determined variationally to be

$$d_{\vec{q}} = \frac{1}{2} \frac{Q(q)(\rho_q + \rho_{-q})}{\omega_q - \vec{v} \cdot \vec{q}}, \quad (4a)$$

with

$$\rho_q = \int d^3r \phi^\dagger(\vec{r}) e^{i\vec{q}\cdot\vec{r}} \phi(\vec{r}). \quad (4b)$$

The wave function  $\phi(\vec{r}_e - \vec{r})$  is taken to be a normalized electronic bound state centered around the lattice distortion. The factor  $e^{i\vec{W}\cdot\vec{r}_e}$  sets the entire system in motion with  $\vec{W}$  determined variationally to be

$$\vec{W} = \vec{v} - \int d^3r \phi^\dagger(\vec{r}) \vec{p} \phi(\vec{r}). \quad (5)$$

The wave function  $|\psi_{\text{sc}}\rangle$  is not an eigenfunction of the total momentum operator

$$\vec{\mathcal{P}} = \vec{p} + \sum_{\vec{q}} \vec{q} a_{\vec{q}}^\dagger a_{\vec{q}}. \quad (6)$$

Rather, the momentum  $\vec{P}$  is introduced as a constraint<sup>2</sup>

$$\vec{P} = \langle \psi_{\text{sc}} | \vec{\mathcal{P}} | \psi_{\text{sc}} \rangle. \quad (7)$$

This is accomplished with the use of a Lagrange multiplier which turns out to be the polaron velocity  $\vec{v}$ .

Solving for the energy in the state  $|\psi_{\text{sc}}\rangle$ , a self-consistent eigenvalue problem results for  $\phi(\vec{r})$ . However, this problem is difficult and it is customary to approximate the solution by

$$\phi(\vec{r}) = (2/\pi\beta^2)^{3/4} e^{-|\vec{r}|^2/\beta^2}. \quad (8)$$

The parameter  $\beta$  is found variationally to be

$$\beta(v) = 3\sqrt{\pi} v/\alpha \ln \left| \frac{1+v}{1-v} \right|. \quad (9)$$

The energy is then given by<sup>2</sup>

$$E_{\text{sc}} = \frac{1}{2}P^2 - \frac{1}{2}(\vec{v} - \vec{P})^2 + \frac{1}{2} \int d^3r \phi^\dagger p^2 \phi - \sum_{\vec{q}} \left( \frac{4\pi\alpha}{vq} \right) \frac{(\text{Re } \rho_q)^2}{q - \vec{v} \cdot \vec{q}}, \quad (10)$$

with  $\vec{v}$  determined by the constraint equation

$$\vec{v} = \vec{P} - \sum_{\vec{q}} \left( \frac{4\pi\alpha}{vq} \right) \frac{\vec{q}(\text{Re } \rho_q)^2}{(q - \vec{v} \cdot \vec{q})^2}. \quad (11)$$

These equations are very similar to those obtained for the intermediate-coupling theory [cf. Eqs. (21) and (22) below].

The expected value of the potential in the space described by the lattice wave function is

$$V_{\text{sc}}(\vec{R}) = \langle 0 | e^{S^\dagger(\vec{r})} \left( \frac{H_{\text{int}}}{e} \right) e^{S(\vec{r})} | 0 \rangle = -\frac{2}{e} \sum_{\vec{q}} Q(q) d_{\vec{q}} \cos(\vec{q} \cdot \vec{R}), \quad (12)$$

where  $\vec{R} = \vec{r} - \vec{r}_e$  is the distance from the center of the electronic wave function. Note that there is symmetry in the forward and backward directions and that the problem possesses cylindrical symmetry around the direction of the polaron velocity. Using the geometry in Fig. 1, where  $\theta$  is the angle between  $\vec{R}$  and  $\vec{v}$ , Eq. (12) reduces to

$$V_{\text{sc}}(\vec{R}, \theta) = -\left(\frac{2}{\pi}\right)^{1/2} \frac{2\alpha}{\beta e} \int_{-1}^1 \frac{d(\cos\theta') e^{-R^2 \cos^2\theta'/\beta^2}}{[(1-v\cos\theta \cos\theta')^2 - v^2 \sin^2\theta \sin^2\theta']^{1/2}}. \quad (13)$$

For  $v=0$ , Eq. (13) yields

$$V_{\text{sc}}(R) = -(2\alpha/R) \text{erf}(\sqrt{2}R/\beta), \quad (14)$$

which gives spherically symmetric potential surfaces as we would expect.

For  $v \neq 0$  the numerical evaluation of Eq. (13) presents little difficulty, although care must be exercised as  $v \rightarrow 1$  because the integrand diverges for  $\theta = \theta'$  when  $v=1$ . This divergence can be traced to  $d_{\vec{q}}$ , which diverges for all values of  $\vec{q}$ . Hence,

the point  $q=0$  plays no special role here as it does in the intermediate-coupling theory.

The surfaces of constant potential now become flattened in the forward and backward directions. Constant potential contours are given in Fig. 2 for  $\alpha=5$  and for  $v=0.0, 0.9$ , and  $0.99$ . For those contours shown the radii of the circles and the minor axes of the elliptical-like contours are equal as one moves outward from the centers. These distances were chosen as 0.125, 0.250, and 0.500,

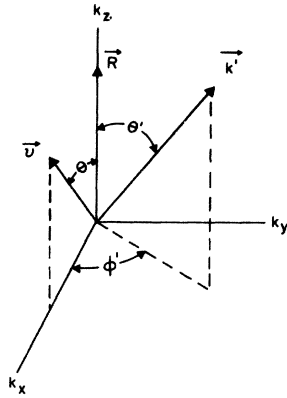


FIG. 1. Geometry for integration of the lattice potential. Because of the cylindrical symmetry in the direction of motion,  $\vec{v}$  can be taken to lie in the  $k_x - k_z$  plane.

respectively. (For CdS, our units are such that  $R = 1$  corresponds to  $\sim 2000 \text{ \AA}$ .) For a constant value of the minor axis the potentials increase in magnitude for small  $R$  as  $v \rightarrow 1$ , but this ceases to be true at larger  $R$  (note crossing of curves for  $V_{||}$  below). Note that the center of the electronic wave function coincides with the center of the potential surfaces and that these surfaces become increasingly more "pancake shaped" as  $v \rightarrow 1$ .

We find that at large distances from the electron the potential

$$V_{sc} \rightarrow -\frac{2\alpha}{eR} \frac{1}{(1 - v^2 \sin^2 \theta)^{1/2}}, \quad R \gg \beta(v), \quad (15)$$

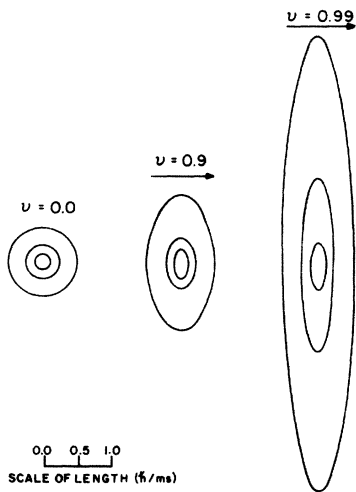


FIG. 2. Constant potential contours in the strong-coupling theory ( $\alpha = 5$ ). The constant potential surfaces are generated by revolving these contours about an axis parallel to  $v$ . The center of the electronic wave function coincides with the center of the contours (surfaces).

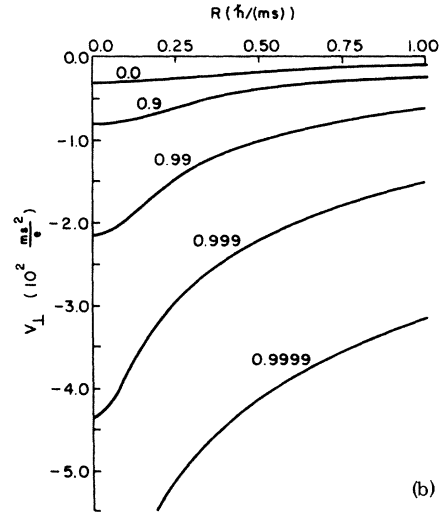
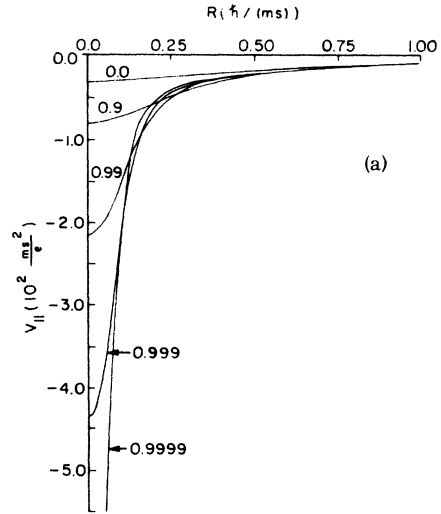


FIG. 3. (a)  $V_{||}$  (strong coupling,  $\alpha = 5$ ) vs the distance from the center of the lattice distortion for various values of  $v \rightarrow 1$ . (b)  $V_{\perp}$  (strong coupling,  $\alpha = 5$ ) vs the distance from the center of the lattice distortion for various values of  $v \rightarrow 1$ .

which on restoring units becomes

$$-\frac{2\alpha \hbar s}{eR} \frac{1}{[1 - (v^2/s^2) \sin^2 \theta]^{1/2}}. \quad (16)$$

This has the same form as the Lienard-Wiechert potential with  $s$  replacing the speed of light. This result is not surprising because  $V_{sc}$  and the Liénard-Wiechert potentials result as solutions of the inhomogeneous wave equation. This is true of  $V_{sc}$  because the strong-coupling polaron theory treats the lattice in a non-quantum-mechanical approximation.

To study these potentials further we define

$$V_{||} \equiv V_{sc}(R, \theta = 0), \quad (17)$$

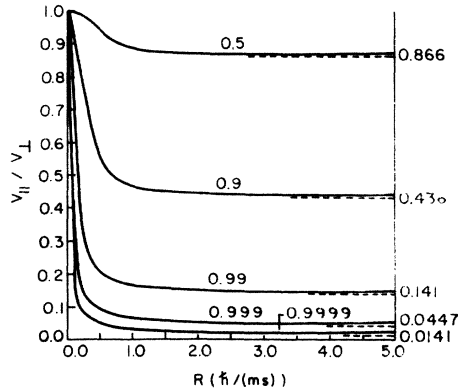


FIG. 4.  $V_{||}/V_{\perp}$  (strong coupling,  $\alpha=5$ ) vs the distance from the center of the lattice distortion for various values of  $v \rightarrow 1$ .

i. e.,  $V_{SC}$  in the direction parallel to  $v$ ; and

$$V_{\perp} \equiv V_{SC}(R, \theta = \frac{1}{2}\pi). \quad (18)$$

i. e.,  $V_{SC}$  in the direction normal to  $v$ . Curves for  $V_{||}$  and  $V_{\perp}$  are given in Figs. 3(a) and 3(b) for  $\alpha = 5$ . It is seen that the potentials diverge at  $R=0$  as  $v \rightarrow 1$ . It is clear that  $V_{||}$  and  $V_{\perp}$  differ considerably even for distances relatively near the center of the lattice distortion. The ratio  $V_{||}/V_{\perp}$  vs  $R$  is shown in Fig. 4. For each  $v$  the ratio  $V_{||}/V_{\perp}$  approaches a limiting value some distance away from the center of the lattice distortion in agreement with Eq. (15).

In Fig. 3(a), it is seen that the curves for  $V_{||}$  cross for different values of  $v$ . This effect can be traced to the collapse of the electronic wave function as  $v \rightarrow 1$  [cf. Eq. (9)]. The electronic and lattice wave functions are treated self-consistently in strong coupling. As  $v$  increases the lattice distortion grows larger causing the electronic radius to become smaller which in turn causes the lattice distortion to become narrower. This eventually leads to the crossings in Fig. 3(a).

Increasing  $\alpha$  in this theory causes the potentials to become deeper as expected. However, increasing  $\alpha$  also causes the potentials to become narrower and forces  $V_{SC}$  to assume the form in Eq. (15) for smaller values of  $R$ .

$$F(\theta', \phi'; \theta) = (c\mu - c\zeta) \cos\zeta + (s\mu - s\zeta) \sin\zeta, \quad \cos\theta' \neq 0$$

$$= \ln \left| \frac{\frac{1}{2}q_m + 1 - v \sin\theta \cos\phi'}{1 - v \sin\theta \cos\phi'} \right|, \quad \cos\theta' = 0 \quad (24b)$$

with

$$\mu = 2R \cos\theta' \left[ \frac{1}{2}q_m + 1 - v (\sin\theta \sin\theta' \cos\phi' + \cos\theta \cos\theta') \right], \quad (24c)$$

and

### B. Intermediate-coupling theory

The trial wave function used in the intermediate-coupling theory is

$$|\Psi_I\rangle = T_1 T_2 |0\rangle, \quad (19a)$$

where

$$T_1 = \exp \left[ -i \left( \sum_{\vec{q}} \vec{q} a_{\vec{q}}^{\dagger} a_{\vec{q}} \right) \cdot \vec{r} \right] \quad (19b)$$

and

$$T_2 = \exp \left( \sum_{\vec{q}} f_{\vec{q}} (a_{\vec{q}}^{\dagger} - a_{\vec{q}}) \right). \quad (19c)$$

The  $f_{\vec{q}}$  are variational parameters given by

$$f_{\vec{q}} = - \frac{Q(q)}{\frac{1}{2}q^2 + q - \vec{q} \cdot \vec{v}}. \quad (20)$$

This wave function is an eigenstate of  $\vec{\sigma}$ . Thus, the energy is an upper bound for each value of  $\vec{P}$  and is given by<sup>1</sup>

$$E_I = \frac{1}{2}P^2 - \frac{1}{2}(\vec{P} - \vec{v})^2 - \sum_{\vec{q}} \left( \frac{4\pi\alpha}{vq} \right) \frac{1}{\frac{1}{2}q^2 + q - \vec{q} \cdot \vec{v}}, \quad (21)$$

with  $\vec{v}$  given by

$$\vec{v} = \vec{P} - \sum_{\vec{q}} \left( \frac{4\pi\alpha}{vq} \right) \frac{\vec{q}}{(\frac{1}{2}q^2 + q - \vec{q} \cdot \vec{v})^2}. \quad (22)$$

Note the similarity between these equations and those obtained in strong coupling [Eqs. (10) and (11)].

The expected value of the lattice potential in the intermediate-coupling theory is

$$V_I = \langle \Psi_I | \frac{H_{int}}{e} | \Psi_I \rangle = \frac{2}{e} \sum_{\vec{q}} Q(q) f_{\vec{q}} \cos(\vec{q} \cdot \vec{R}), \quad (23)$$

where  $\vec{R}$  is the distance from the electron site. The same symmetries hold here as in the strong-coupling theory. Using the geometry in Fig. 1, Eq. (23) reduces to

$$V_I(R, \theta) = - \frac{2\alpha}{e\pi^2} \int_0^{2\pi} d\phi' \int_{-1}^1 d(\cos\theta') F(\theta', \phi'; \theta), \quad (24a)$$

where

$$\zeta = 2R \cos\theta' [1 - v(\sin\theta \sin\theta' \cos\phi' + \cos\theta \cos\theta')] . \tag{24d}$$

The functions si and ci are the sine and cosine integrals.<sup>13</sup> In our units, the maximum wave vector is  $q_m \approx 300$ . Note, from Eq. (24), that the coupling constant in this theory affects the potential only as a multiplicative factor.

For  $v = 0$ , Eq. (24) yields

$$V_I(R) = -\left(\frac{4\alpha}{\pi e}\right) \frac{1}{R} \left\{ \sin(2R) \text{ci}[(q_m + 2)R] - \cos(2R) \text{si}[(q_m + 2)R] + \cos(2R) \text{si}(2R) - \sin(2R) \text{ci}(2R) + \text{si}(q_m R) + \frac{1}{2}\pi \right\}, \quad v = 0 . \tag{25}$$

Note for  $R \rightarrow \infty$

$$V_I(R) \rightarrow -2\alpha/eR, \quad v = 0 \tag{26}$$

as in strong coupling [cf. Eq. (15)].

For  $v \neq 0$ , Eq. (24) can be evaluated numerically.<sup>14</sup> Here also care must be exercised in the limit  $v \rightarrow 1$  because the integrand diverges for  $\theta = \theta'$  when  $v = 1$  [ci(x)  $\rightarrow \infty$  as  $x \rightarrow 0$ ]. In these integrals small wave vectors play a dominant role. However, it was shown before<sup>4</sup> that the system has the same qualitative behavior if we cut off the interaction at small  $q$ . Also, that the strong-coupling theory makes no special use of the  $q \approx 0$  phonons suggests they are not essential to produce the anomaly that we are concerned with here.

The contours corresponding to the constant potential surfaces are given in Fig. 5 for  $v = 0.0, 0.9$ , and  $0.99$ . For those contours shown, the radii of the circular contours and the minor axes of the elliptical-like contours are equal as one moves outward from the centers. These distances were chosen as 2.5, 5.0, and 10.0 (note, the scale of length is 20 times that in Fig. 2). As  $v$  increases the potentials increase in magnitude for a constant value of the minor axis. Note that the

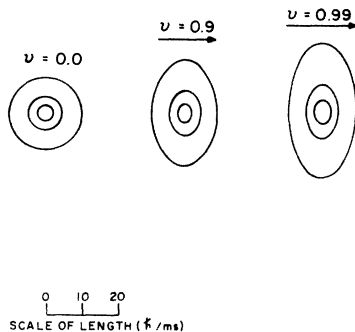


FIG. 5. Constant potential contours in the intermediate-coupling theory.

electron is at the very center of these contours (surfaces).

Potentials  $V_{||}$  and  $V_{\perp}$  can be defined similar to Eqs. (17) and (18). The curves for  $V_{||}$  are given in Fig. 6 for  $R$  relatively close to the electron site. The curves for  $V_{\perp}$  are approximately the same as those for  $V_{||}$  at these distances. For  $R \rightarrow \infty$ ,  $V_{||} \rightarrow A/R$  and  $V_{\perp} \rightarrow B/R$  to first order in  $1/R$ . We could not determine the parameters  $A$  and  $B$ , both of which appear to be functions of velocity. The ratio  $V_{||}/V_{\perp}$  vs  $R$  is shown in Fig. 7. It can be seen that  $V_{||}$  and  $V_{\perp}$  differ for large  $R$ . It is clear that the potential surfaces in intermediate coupling have the same qualitative behavior as in strong coupling except that the flattening occurs at larger distances from the electron because of the emphasis of the long-wavelength phonons in this theory. The potentials do not approach the Lié-nard-Wiechert form at large  $R$  because the intermediate-coupling theory does not treat the lattice classically as the strong-coupling theory does.

### III. DISCUSSION

The conclusion drawn from the preceding calculations is that in both the strong-coupling and inter-

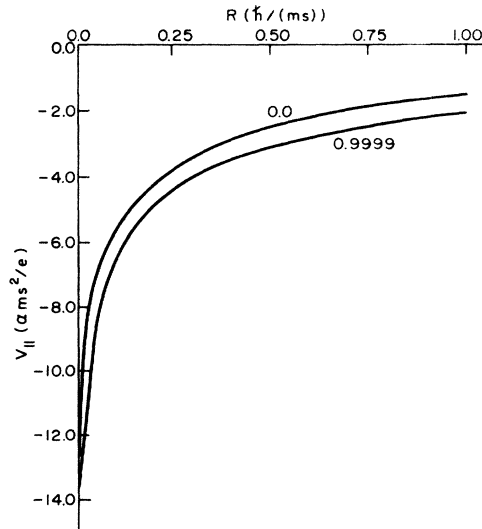


FIG. 6.  $V_{||}$  (intermediate coupling) vs the distance from the center of the lattice distortion for  $v = 0.0$  and  $v = 0.9999$ . (The coupling constant is  $\alpha$ .) The curves of  $V_{||}$  for intermediate values of  $v$  lie between these two curves. The curves of  $V_{\perp}$  vs  $R$  are approximately the same as those of  $V_{||}$  for this range of  $R$ .

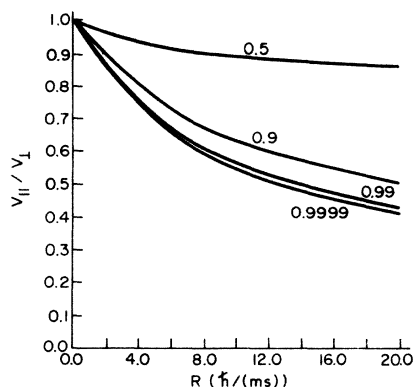


FIG. 7.  $V_{||}/V_1$  (intermediate coupling) vs distance from the center of the lattice distortion for various values of  $v$ .

mediate-coupling theories the electron continues to be "clothed" by its concomitant lattice distortion even as the polaron velocity approaches the speed of sound. In fact, the lattice potential around the electron deepens as  $v \rightarrow s$ , indicating that the lattice distortion grows larger in this limit.

Although the strong-coupling theory requires larger values of  $\alpha$  than are known for existing piezoelectric crystals, the theory is very useful in the present context because it shows very clear-

ly what is happening to the polaron as it approaches the speed of sound. As  $v \rightarrow 1$  the lattice potential flattens in the direction of motion and becomes much deeper pulling the electron into the central region which is still spherical. This in part explains why when a "pancake-shaped" electron wave function was used in a previous work,<sup>2</sup> only a slight lowering of the energy was obtained.

The behavior in the intermediate-coupling theory is roughly the same as for strong coupling except that since the interaction with long-wavelength phonons is emphasized, the flattening takes place at larger distances from the center of the lattice distortion (from the electron site).

As has been mentioned previously<sup>2</sup> it is interesting to note that since the lattice distortion grows as the polaron velocity approaches the speed of sound, one would expect that the strong-coupling theory would be favored at high velocity even in cases where weak coupling is better at  $v = 0$ .

#### ACKNOWLEDGMENTS

We wish to thank Dr. M. Rona of the Middle-East Technical University and Dr. James Licari for their comments concerning this work. We also thank Michael Duffy for a helpful suggestion concerning the computer programming.

<sup>1</sup>George Whitfield, J. Gerstner, and K. Tharmalingam, *Phys. Rev.* **165**, 993 (1968).

<sup>2</sup>R. Parker, George Whitfield, and M. Rona, *Phys. Rev. B* **10**, 698 (1974).

<sup>3</sup>James J. Licari and George Whitfield, *Phys. Rev. B* **9**, 1432 (1974).

<sup>4</sup>M. Rona and George Whitfield, *Phys. Rev. B* **7**, 2727 (1973).

<sup>5</sup>Meheryar Engineer and George Whitfield, *J. Phys. Soc. Jpn.* **34**, 564 (1973).

<sup>6</sup>John Thomchick and George Whitfield, *Phys. Rev. B* **9**, 1506 (1974).

<sup>7</sup>T. D. Schultz, Solid State and Molecular Theory Group, MIT Technical Report No. 9, 1956 (unpublished).

<sup>8</sup>T. D. Lee, F. Low, and D. Pines, *Phys. Rev.* **90**, 297 (1953).

<sup>9</sup>M. Gurari, *Philos. Mag.* **44**, 329 (1953).

<sup>10</sup>S. I. Pekar, *Research in Electron Theory of Crystals*, U. S. Atomic Energy Commission (U. S. GPO, Washington, D. C., 1963).

<sup>11</sup>A. R. Hutson, *J. Appl. Phys.* **32**, 2287 (1961).

<sup>12</sup>G. D. Mahan, in *Polarons in Ionic Crystals and Polar Semiconductors*, edited by Jozef T. Devreese (Elsevier, New York, 1972).

<sup>13</sup>The sine integral is  $\text{si}(z) = -\int_z^\infty \frac{(\sin t)/t}{t} dt$  ( $|\arg z| < \pi$ ); the cosine integral is  $\text{ci}(z) = -\int_z^\infty \frac{(\cos t)/t}{t} dt$  ( $|\arg z| < \pi$ ). See *Handbook of Mathematical Functions*, Natl. Bur. Stds. Appl. Math. Ser. 55 (U. S. GPO, Washington, D. C., 1964).

<sup>14</sup>For the numerical evaluation of  $\text{si}$  and  $\text{ci}$ , see Jet Wimp, *Math. Comput.* **15**, 174 (1961).